191

NASA TECHNICAL NOTE

NASA TN D-574

NASA TN D-574

KINEMATIC ANALYSIS OF THE ENGINE AND PUMP INLET DUCT GIMBAL JOINT SYSTEM IN THE S-1C STAGE OF THE SATURN V VEHICLE

by F. F. Garcia

George C. Marshall Space Flight Center
Huntsville, Ala.

NATIONAL AERONAUTICS AND SPACE ADMINISTRATION • WASHINGTON, D. C. • OCTOBER 1964

KINEMATIC ANALYSIS OF THE ENGINE AND PUMP INLET DUCT GIMBAL JOINT SYSTEM IN THE S-IC STAGE OF THE SATURN V VEHICLE

By F. F. Garcia

George C. Marshall Space Flight Center
Huntsville, Ala.

NATIONAL AERONAUTICS AND SPACE ADMINISTRATION

For sale by the Office of Technical Services, Department of Commerce,
Washington, D.C. 20230 -- Price $1.25

TABLE OF CONTENTS

LIST OF ILLUSTRATIONS

SECTION II

APPENDIX A

APPENDIX B

LIST OF ILLUSTRATIONS (Concluded)

DEFINITION OF SYMBOLS

Symbol	Definition
A_e	Engine gimbal angle about gimbal axis rigid to engine.
A_v	Engine gimbal angle about gimbal axis rigid to vehicle.
A_{ev}	Resultant angle of rotation of engine about the gimbal axes.
B	Horizontal distance of duct aft gimbal center from engine gimbal center along a line normal to the engine gimbal axis when engine is at zero gimbal position.
C	Vertical distance of duct aft gimbal center from engine gimbal center when engine is at zero gimbal position.
E	Vertical distance of duct aft gimbal center from forward gimbal center after engine gimbaling.
H	Vertical distance of duct forward gimbal center from engine gimbal center.
L	Distance of duct aft gimbal center from forward gimbal center or effective length of the duct.
R	The length of the horizontal component of $a_{a2}a'_{a2}$ projected on the right auxiliary projection plane.
S	The length of the horizontal component of $a_{a2}a'_{a2}$ projected on a plane normal to the right auxiliary projection plane.
Y	The length of the horizontal component of $a_{a2}a'_{a2}$ projected on the rear projection plane.
Z	The length of the horizontal component of $a_{a2}a'_{a2}$ projected on the right projection plane.
$a_a a'_a$	Duct aft gimbal axis of unit length and is rigid to the engine.

DEFINITION OF SYMBOLS (Continued)

Symbol	Definition
$b_a b'_a$	Duct aft gimbal axis of unit length and is movable with respect to the engine.
$a_f a'_f$	Duct forward gimbal axis of unit length and is rigid to the vehicle.
$b_f b'_f$	Duct forward gimbal axis of unit length and is movable with respect to the vehicle.
α	Angle between $a_{ao} a'_{ao}$ and the engine gimbal axis that is rigid to the vehicle.
β	Angle between duct longitudinal axis and its vertical component after engine gimbaling.
γ	Angle between $a_{fo} a_{fo}$ and the horizontal component of the duct longitudinal axis.
δ	Angle between the horizontal components of $b_{a2} b'_{a2}$ and the duct longitudinal axis.
ζ	Angle between $b_{fo} b'_{fo}$ and the engine gimbal axis that is rigid to the vehicle.
η	Angle between the horizontal components of the duct longitudinal axis and pump inlet centerline.
θ	Angle between $b_{ao} b'_{ao}$ and $b_{fo} b'_{fo}$
θ'	Angle between $b_{a2} b'_{a2}$ and $b_{f2} b'_{f2}$
λ	Angle between the plane containing $a_{f2} a'_{f2}$ and the vertical plane both of which intersect at the duct longitudinal axis after engine gimbaling.
μ	Angular deflection in bending of the duct aft gimbal joint after engine gimbaling.
σ	The angle which the horizontal component of $a_{a2} a'_{a2}$ makes with the engine gimbal axis that is rigid to the vehicle.

DEFINITION OF SYMBOLS (Concluded)

Symbol	Definition
τ	Torsional deflection or twist angle of the duct due to engine gimbaling.
ϕ	Angle between the plane containing $b_{a2}b'_{a2}$ and the vertical plane both of which intersect at the duct longitudinal axis after engine gimbaling.
ω	Angle between the horizontal component of the duct longitudinal axis and the engine gimbal axis that is rigid to the vehicle.

Subscripts

e	Pertaining to engine gimbal axis that is rigid to the engine.
v	Pertaining to engine gimbal axis that is rigid to the vehicle.
0, 1, 2	Pertain to engine gimbal position.

TECHNICAL NOTE

KINEMATIC ANALYSIS OF THE ENGINE AND PUMP INLET DUCT GIMBAL JOINT SYSTEM IN THE S-IC STAGE OF THE SATURN V VEHICLE

SUMMARY

A mathematical simulator of the engine and pump inlet duct gimbal joint system in the S-IC stage of the SATURN V vehicle was developed as a result of the kinematic analysis conducted. The simulator provided a convenient means and a precise method for determining the torsional, longitudinal, and bending deflections of the pump inlet ducts when the engine is gimbaled to its maximum limits.

It is concluded that the torsional deflection of the pump inlet ducts in the S-IC stage of the SATURN V vehicle can be made to equal zero or can be reduced considerably by proper orientation of the three gimbal joints.

It is recommended that the proper combination of deflections determined from this analysis be used in the evaluation of the overall loading conditions at the pump inlet; and that the pump inlet ducts gimbal joints in the S-IC stage of the SATURN V vehicle be oriented to eliminate or minimize the torsional deflection load.

SECTION I. INTRODUCTION

A well defined engine to stage interface design criteria is required to insure the design compatibility and adequacy of the affected components. During review of the F-1 engine pump inlet and duct loading conditions in the S-IC stage of the SATURN V vehicle, there was a problem in meeting the load conditions imposed by the engine; or conversely, there was a problem in meeting the load conditions imposed by the pump inlet duct. One area of incompatibility was in the torsional load component; consequently the validity of the established requirement was questioned. It was found that a better understanding of the pump inlet duct deflections, especially the torsional deflection, was required to properly establish more realistic pump inlet duct deflection load components. Consequently, a kinematic analysis of the system was undertaken.

The intent of this report is to describe, in detail, the kinematic analysis conducted, the mathematical simulator developed, and the results obtained. In this analysis, the gimbal joints supports and engine structures were treated as rigid members, and the gimbal joints slop was not considered. The deflections obtained are therefore due to pure engine gimbal movements only.

The relationships for the torsional and longitudinal deflections of the duct shown in Section II and Appendix A of this report are the same as those covered in Reference 1 although some of the expressions have been simplified. The exact relationship for the angular deflection in bending of the duct aft gimbal joint replaced the corresponding approximate expression in Reference 1. It is noteworthy, however, that for the magnitude of gimbal angles used in the S-IC stage, the bending deflection obtained from the approximate expression is within three hundredths of one per cent of that obtained from the exact relationship. The results shown in this report are based on the nominal system design parameters verified to be the latest to date. These results differ very slightly from the preliminary results reported in Reference 1 and is attributed to the difference in the initial orientation angle used for the duct aft gimbal joint.

SECTION II. DESCRIPTION

The deflections of the pump inlet duct due to engine gimbal movement are expressed as indicated below. These equations were derived as explained in Appendix A. Figures 1 and 2 show the typical parameters and variables in schematic diagram. Although only the LOX system is represented in the diagrams, the equations are applicable to the fuel systems as well as any other three universal joint type linkage that is subjected to motions similar to the system studied.

The general equation for torsional deflection, τ or twist of the duct is

$$\tau = \mathrm{Tan}^{-1}\left[\mathrm{Cos}\,\beta\ \mathrm{Tan}\,\delta\right] - \mathrm{Tan}^{-1}\left[\frac{\mathrm{Tan}(\omega+\zeta-90)}{\mathrm{Cos}\,\beta}\right] - (\alpha-\zeta) \qquad (9)^*$$

where

$$\mathrm{Cos}\,\beta = \frac{E_2}{L_2} \qquad (21)$$

$$\mathrm{Tan}\,\delta = \frac{WZ - XY}{XZ + WY} \qquad (38)$$

$$\mathrm{Tan}\,\omega = \frac{W}{X} \qquad (19)$$

$$E_2 = H - B_v \mathrm{Sin}\,A_v - \mathrm{Cos}\,A_v\,(B_e \mathrm{Sin} A_e + C\,\mathrm{Cos} A_e) \qquad (14)$$

$$L_2 = (E_2^2 + W^2 + X^2)^{\frac{1}{2}} \qquad (24)$$

$$W = B_v\,(1 - \mathrm{Cos}\,A_v) + \mathrm{Sin}\,A_v\,(B_e \mathrm{Sin}\,A_e + C\,\mathrm{Cos}\,A_e) \qquad (18)$$

$$X = B_e\,(1 - \mathrm{Cos}\,A_e) + C\,\mathrm{Sin}\,A_e \qquad (20)$$

$$Y = \mathrm{Cos}\,\alpha \mathrm{Cos}\,A_e \qquad (26)$$

$$Z = \mathrm{Cos}\,A_v\,\mathrm{Sin}\alpha + \mathrm{Sin}\,A_v\,\mathrm{Sin}\,A_e\,\mathrm{Cos}\,\alpha \qquad (31)$$

The general equation for longitudinal deflection, ΔL, or change in length of the duct is

$$\Delta L = L_2 - L_o \qquad (25)$$

---

* The equation sequence here is taken from Appendix A starting on page 13 of this report.

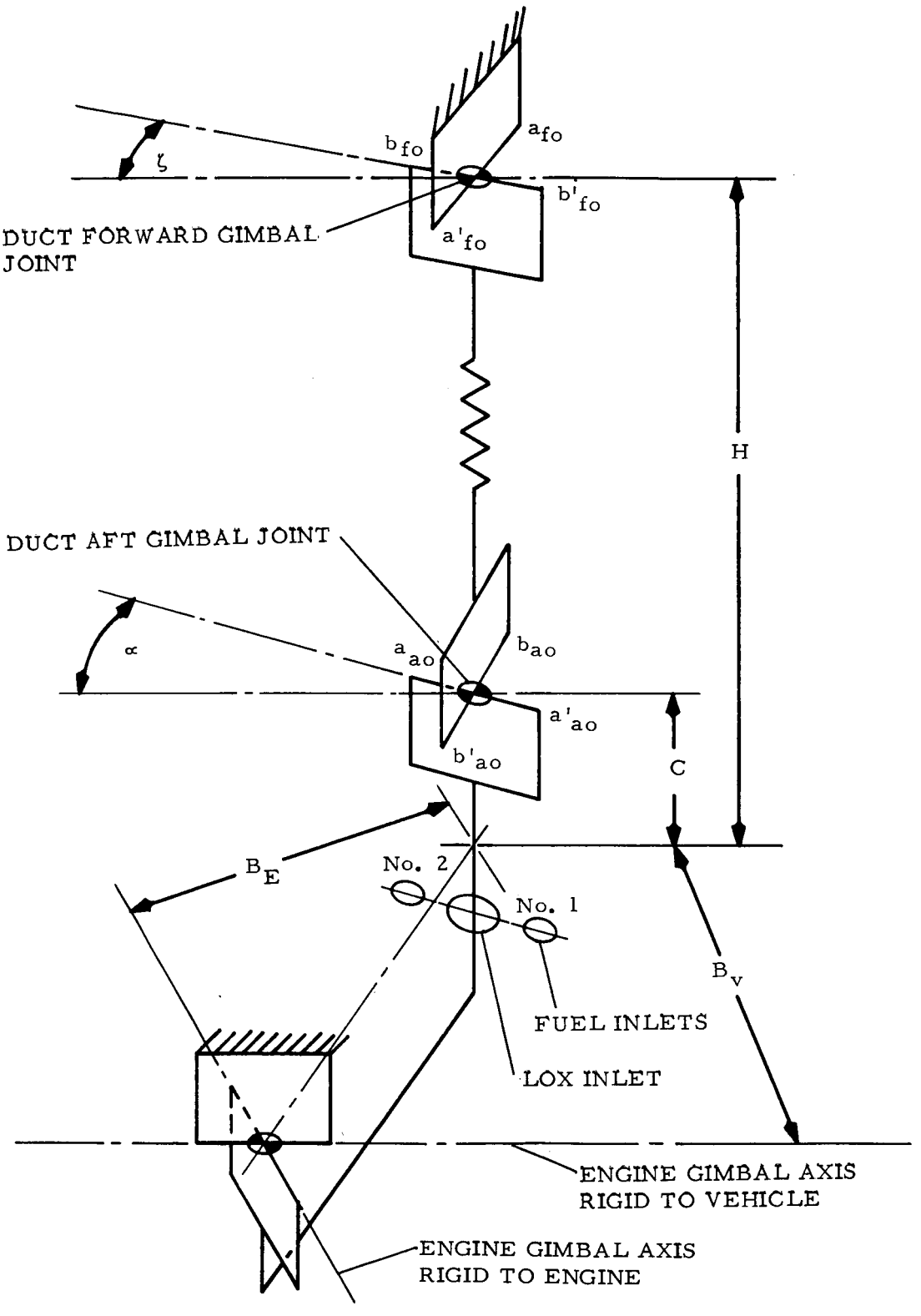

FIGURE 1. F-1 ENGINE AND PUMP INLET DUCT GIMBAL JOINTS SYSTEM SCHEMATIC (ZERO GIMBAL POSITION)

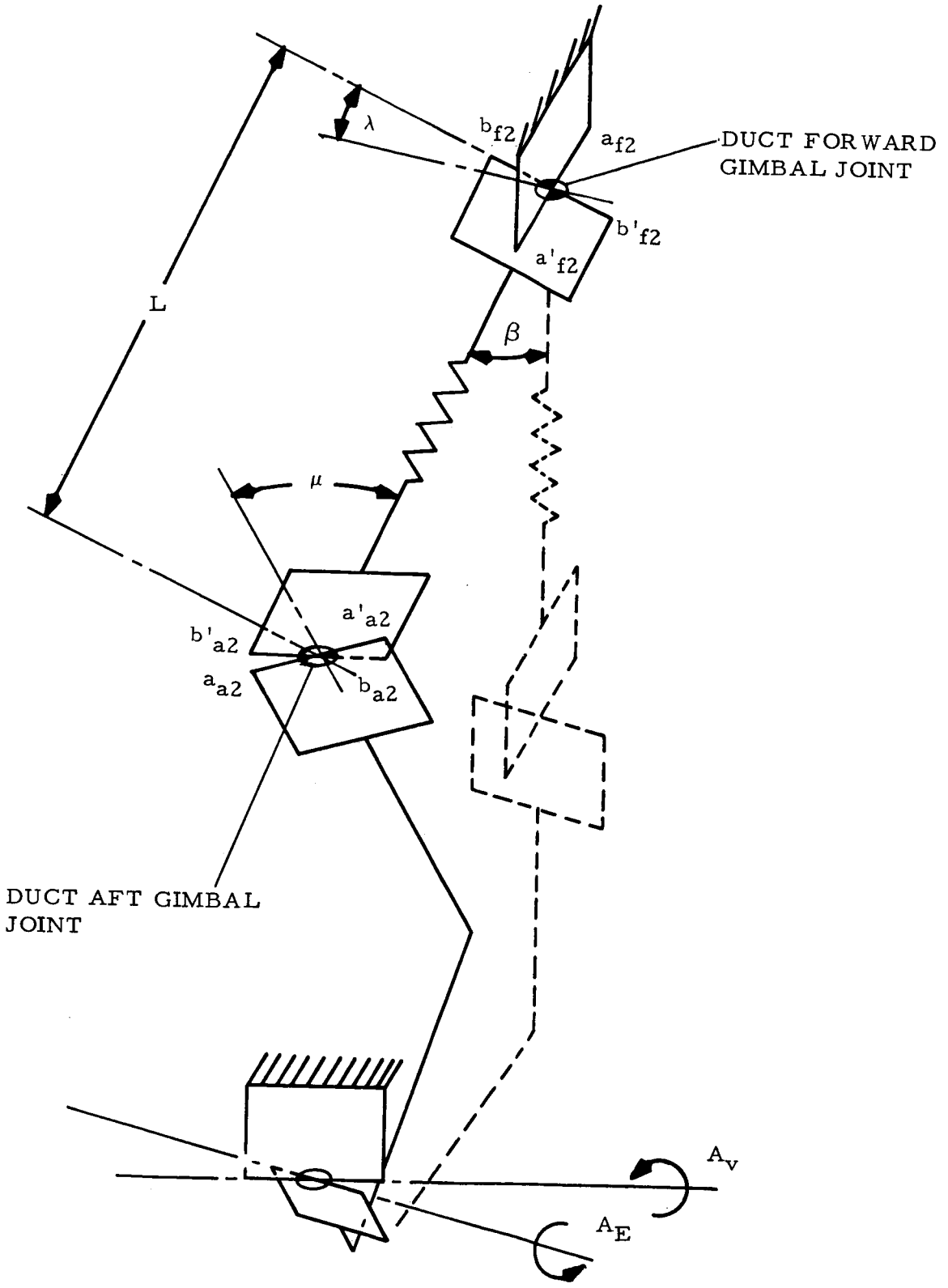

FIGURE 2. F-1 ENGINE AND PUMP INLET DUCT GIMBAL JOINTS SYSTEM SCHEMATIC (GIMBALED POSITION)

where L_2 is the same expression as Eq. (24) and L_o is the effective duct length when the engine gimbal angles A_v and A_e are equal to zero.

The general equation for angular deflection in bending, μ, of the duct aft gimbal joint is

$$\mu = \text{Cos}^{-1} (\text{Cos } \beta \text{ Cos } A_{ev} - \text{Sin } \beta \text{ Sin } A_{ev} \text{ Cos} \eta) \tag{50}$$

where

$$A_{ev} = \text{Cos}^{-1}(\text{Cos } A_e \text{ Cos } A_v) \tag{54}$$

$$\eta = \omega - \text{Tan}^{-1}\left(\frac{\text{Sin } A_v}{\text{Tan } A_e}\right) \tag{58}$$

and angles β and ω are those obtained from Eqs. (21) and (19) respectively.

SECTION III S-IC STAGE SYSTEM

The curves shown on Figures B-1 through B-9 in Appendix B represent the solutions to the equations in Section II when applied to the gimbal joint system arrangement in the S-IC stage. The values assigned to the parameters are shown on Table I. These were obtained from References 2 through 8. Combinations of engine gimbal angles that define the maximum limits for 6 degree circular and square patterns were assigned to the variables A_e and A_v; thus, the maximum deflections throughout these gimbal ranges were obtained. Noting the definition of ω, the curves therefore indicate the deflections of the ducts at the directional positions of the duct aft gimbal center after gimbaling the engine to the defined limits.

Figures B-10 through B-12 are graphical representations of the relationship between ω and the combinations of A_e and A_v for 6 degree circular as well as square engine gimbal pattern. Negative engine gimbal angle indicates that the duct aft gimbal center is displaced toward aft. Conversely, positive engine gimbal angle indicates that the duct aft gimbal center is displaced forward.

To determine the gimbal angle combination that produces a certain magnitude of deflection, or vice versa, Figures B-10 through B-12 are used

in conjunction with Figures B-1 through B-9. For example, Figure B-1 indicates that for a 6 degree circular engine gimbal pattern the maximum torsional deflection of plus 14.1 minutes occurs when the LOX duct aft gimbal center is on the direction angle ω of plus 26 degrees. From Figure B-10, the corresponding combination of engine gimbal angles is found to be plus 5.5 and plus 2.4 degrees for A_e and A_v respectively. Also at this compound gimbal angle the change in length, ΔL, of the duct is minus 4.8 inches as indicated in Figure B-4, and the angular deflection, μ, of the duct aft gimbal joint is 7.9 degrees as indicated in Figure B-7. As shown by the curves, the motions and the resulting deflections of the ducts are non-symetrical. Also, the deflections to which the ducts are concurrently subjected are not identical. This is due to the motions governing universal joints, and the difference is geometry of the systems.

Table II shows a summary of the deflection data obtained. It is reiterated that these deflections are the results of pure engine gimbal movements only.

TABLE I Systems Design Parameters (Nominal).

		SYSTEM		
		FUEL NO. 1	LOX	FUEL NO. 2
C,	Inches	8.715	16.118	8.715
B_e,	Inches	53.6435	35.3555	17.0675
B_v,	Inches	17.0675	35.3555	53.6435
H,	Inches	69.045	80.168	69.045
L_o,	Inches	60.330	64.050	60.330
α,	Degrees	+45.00	+45.00	+45.00
ζ,	Degrees	-15.00	-15.00	-15.00

TABLE II Summary of F-1 Engine Pump Inlet Duct Deflections Due to Engine Gimbaling For α = +45 and ζ = -15 Degrees

	CIRCULAR GIMBAL PATTERN			SQUARE GIMBAL PATTERN		
	No. 1 Fuel	LOX	No. 2 Fuel	No. 1 Fuel	LOX	No. 2 Fuel
τ max, minutes	+13.7	+14.1	-13.6	-19.8	+20.5	-19.4
ΔL, inches	-5.8	-4.7	-4.6	-3.5	-7.1	-3.5
μ, degrees	7.3	7.9	7.1	10.4	11.4	9.8
ω, degrees	+27	+26	+108	-49	+50	+129
A_e/A_v, degrees	+5.5/+2.3	+5.5/+2.4	-2.4/+5.5	+6.0/-6.0	+6.0/+6.0	-6.0/+6.0
$-\Delta L$ max, inches	5.8	5.1	5.8	7.2	7.1	7.2
τ, minutes	+13.7	+10.3	-1.4	+19.0	+20.5	+19.3
μ, degrees	7.3	7.9	7.3	10.6	11.4	10.4
ω, degrees	+24	+49	+75	+53	+50	+54
A_e/A_v, Degrees	+5.7/+2.0	+4.2/+4.2	+2.0/+5.7	+6.0/+6.0	+6.0/+6.0	+6.0/+6.0
$+\Delta L$ max, inches	5.9	5.3	5.9	7.5	7.5	7.5
τ, minutes	+13.3	+9.8	-1.4	+18.8	+19.3	+19.0
μ, degrees	6.6	7.2	6.6	9.1	9.9	9.3
ω, degrees	-170	-141	-119	-160	-144	-152
A_e/A_v, degrees	-5.7/-2.0	-4.2/-4.2	-2.0/-5.7	-6.0/-6.0	-6.0/-6.0	-6.0/-6.0
μ max, degrees	7.3	7.9	7.3	10.6	11.4	10.4
τ, minutes	+13.7	+10.3	-1.4	+19.0	+20.5	+19.3
ΔL, inches	-5.8	-5.1	-5.8	-7.2	-7.1	-7.2
ω, degrees	+24	+49	+75	+53	+50	+54
A_e/A_v, degrees	+5.7/+2.0	+4.2/+4.2	+2.0/+5.7	+6.0/+6.0	+6.0/+6.0	+6.0/+6.0

SECTION IV. ANALYSIS

The general equations in Section II were analyzed to determine means and the feasibility of eliminating or minimizing the pump inlet duct deflections. The equations show that the deflections depend upon the design parameters C, B_e, B_v, H, α and ζ. Obviously, any change to C B_e, B_v, and H would not be feasible in the S-IC stage but should warrant considerations in more advance systems. To illustrate the effects of these parameters let C, B_e and B_v be equal to zero and α be equal to 90 degrees. The general equations in Section II are then reduced to the following relationships:

For Torsional Deflection;

$$W = 0$$

$$X = 0$$

$$Y = 0$$

$$Z = 0$$

$$N = 0$$

$$L_2 = E_2$$

$$\text{Cos } \beta = 1$$

$$\text{Tan } \delta = 0$$

$$\text{Tan } \omega = 0$$

therefore

$$\tau = 0$$

For Longitudinal Deflection;

$$L_2 = L_O$$

therefore

$$\Delta L = 0$$

For Duct aft Gimbal Joint Bending Deflection;

$$B = 0$$

therefore

$$\mu = A_{ev}$$

It is seen that the torsional and longitudinal deflections are completely eliminated but not the angular deflection in bending. The system would therefore be reduced to a single gimbal joint arrangement. The pump inlet duct aft gimbal joint and the engine gimbal would be combined into one joint.

A practicable approach at the present phase of the S-IC stage development would be to change α and/or ζ. By making α equal to 90 degrees and ζ equal to zero, the torsional deflection will be eliminated as shown below. Referring to the general equations for torsional deflection in Section II,

$$Y = 0$$

since

$$\text{Cos } \alpha = 0$$

therefore

$$\text{Tan } \delta = \text{Tan } \omega$$

Eq. (9) is rewritten as follows:

$$\tau = \text{Tan}^{-1}(\text{Cos } \beta \text{ Tan } \omega) - \text{Tan}^{-1} \left[\frac{\text{Tan } (\omega - 90)}{\text{Cos } \beta} \right] - 90$$

The last two terms are simplified to the form,

$$\text{Tan}^{-1} \left[\frac{\text{Tan } (\omega - 90)}{\text{Cos } \beta} \right] - 90 = \text{Tan}^{-1} (\text{Cos } \beta \text{ Tan } \omega)$$

therefore,

$$\tau = 0$$

To accomplish this change, the pump inlet ducts would have to be modified to orient the gimbal joints as required.

Another alternative would be to install the pump inlet duct as it is, but make α equal to 90 degrees. In this arrangement ζ will be equal to 30 degrees. Using these values and those of the other parameters shown in Table I, the curves on Figures B-13 through B-15 of Appendix B were obtained. Comparing these curves with those on Figures B-1 through B-3, it is seen that the torsional deflection is reduced considerably. change to orient the unmodified duct so that ζ is equal to zero and α is equal to 60 degrees would not produce as much reduction in torsional deflection as the former alternative. This indicates the sensitivity of the torsional deflection to the orientation angle α, of the duct aft gimbal joint. Table III shows a summary of overall pump inlet duct deflections at maximum torsion when α is equal to 90 degrees and ζ is equal to 30 degrees. The maximum longitudinal and bending deflections for this set of conditions is the same as those shown in Table II.

SECTION V. CONCLUSIONS AND RECOMMENDATIONS

The kinematic approach in determining the deflections of the pump inlet ducts due to gimbal movements of the F-1 engine in the S-IC vehicle is precise. The duct deflections depend upon the geometry of the system and the orientation of the duct aft and forward gimbal joint axes with respect to the engine gimbal axes. The maximum deflections in torsion, compression, and bending do not necessarily occur concurrently. Maximum tension occurs with some intermediate deflections in torsion and bending. The torsional deflection of the pump inlet ducts due to engine gimbaling can be reduced to zero by orienting the duct aft and forward gimbal joints so that α is equal to 90 degrees and ζ is equal to zero. The general equations stated in Section II are applicable to any three universal joint type linkage subjected to motions similar to those of the F-1 engine and pump inlet duct system of the S-IC vehicle.

As a result of this analysis and in view of the critical pump inlet load requirement, it is recommended that the pump inlet ducts gimbal joints in the S-IC vehicle be oriented to eliminate or minimize the torsional deflection due to engine gimbal movements.

TABLE III Summary of F-1 Engine Pump Inlet Duct Torsional Deflection Due to Engine Gimbaling For $\alpha = +90$ and $\zeta = +30$

	CIRCULAR GIMBAL PATTERN			SQUARE GIMBAL PATTERN		
	No. 1 Fuel	LOX	No. 2 Fuel	No. 1 Fuel	LOX	No. 2 Fuel
τ' max, minutes	+.41	−.94	−.43	−.86	−1.48	−.67
ΔL, inches	−5.2	-4.8	-5.8	-7.2	-7.1	-7.2
μ, degrees	7.3	7.9	7.2	10.6	11.4	10.3
ω, degrees	-14	+73	+77	+53	+50	+54
A_e / A_v, degrees	+5.9/-1.2	+ 2.0/+5.7	+ 1.8/+5.8	+6.0/+6.0	+6.0/+6.0	+6.0/+6.0
τ' max, percent of τ max for present system	3.0	6.7	3.2	4.3	7.2	3.5

APPENDIX A
DERIVATION OF DEFLECTION EQUATIONS

The equations shown in Section II of this report were derived with the aid of the kinematic diagram shown in Figure A-1 (Drawing No. 20SK96). The torsional deflection can be expressed as

$$\tau = \theta - \theta' \tag{1}$$

From the top views of the kinematic diagram, it can be seen that

$$\theta = 90 - \alpha + \zeta \tag{2}$$

$$\theta' = 90 + \lambda - \phi \tag{3}$$

For convenience in developing the diagram, α and ζ were drawn equal and approximately 45 degrees. For the purpose of this derivation, however, α and ζ should be regarded as having any value from zero to 90 degrees. Also, the angles A_e and A_e were exaggerated.

To express λ and ϕ of Eq. (3) as functions of some variables that would better describe the general state of the system and at the same time show correlation with the system design parameters, the subsequent relationships were obtained. From the top view of the diagram, it can be seen that

$$\gamma = \omega - (90 - \zeta) \tag{4}$$

Noting the definition of line segment $a_{f2}a_{f2}'$

$$\lambda = \mathrm{Tan}^{-1}\left[\frac{\mathrm{Sin}\,\gamma}{\mathrm{Cos}\,\gamma\ \mathrm{Cos}\,\beta}\right] \tag{5}$$

Combining Eqs. (4) and (5)

$$\lambda = \mathrm{Tan}^{-1}\left[\frac{\mathrm{Tan}\,(\omega+\zeta-90)}{\mathrm{Cos}\,\beta}\right] \tag{6}$$

Similarly, from the top and right auxiliary views and noting the definition of line segment $b_{a2}b_{a2}'$

$$\mathrm{Tan}\,\delta = \frac{\mathrm{Sin}\,\phi}{\mathrm{Cos}\phi\mathrm{Cos}\,\beta} \tag{7}$$

therefore

$$\phi = \text{Tan}^{-1} (\text{Cos } \beta \text{ Tan } \delta) \tag{8}$$

Combining Eqs. (1), (2), (3), (6), and (8), the general expression for torsional deflection was obtained.

$$\tau = \text{Tan}^{-1} (\text{Cos } \beta \text{ Tan } \delta) - \text{Tan}^{-1} \left[\frac{\text{Tan } (\omega + \zeta - 90)}{\text{Cos } \beta}\right] - (\alpha - \zeta) \tag{9}$$

Negative τ indicates a twist in the counter clockwise direction looking aft.

The variables β, δ, and ω were then expressed in terms of the system design parameters as follows. From the right side and rear auxiliary views, it can be seen that

$$G_1 = B_v \text{ Sin } A_v + C \text{ Cos } A_v \tag{10}$$

$$G_2 = B_e \text{ Sin } A_e + C \text{ Cos } A_e \tag{11}$$

$$E_1 = H - G_1 \tag{12}$$

$$E_2 = E_1 - (G_2 - C) \text{ Cos } A_v \tag{13}$$

Combining Eqs. (10) through (13), the following relationship for E_2 was obtained.

$$E_2 = H - B_v \text{ Sin } A_v - \text{Cos } A_v (B_e \text{ Sin } A_e + C \text{ Cos } A_e) \tag{14}$$

Similarly, from the right side, rear auxiliary, and top views, it can be seen that

$$I_1 = B_v (1 - \text{Cos} A_v) + C \text{ Sin } A_v \tag{15}$$

$$I_2 = (G_2 - C) \text{ Sin } A_v \tag{16}$$

$$W = I_1 + I_2 \tag{17}$$

Combining Eqs. (15) through (17), the following relationship for W was obtained.

$$W = B_v (1 - \mathrm{Cos}A_v) + \mathrm{Sin}A_v (B_e \mathrm{Sin}A_e + C \mathrm{Cos}A_e) \tag{18}$$

From the top and rear auxiliary views, it can be seen that

$$\mathrm{Tan}\ \omega = \frac{W}{X} \tag{19}$$

where

$$X = B_e (1 - \mathrm{Cos}A_e) + C \mathrm{Sin}\ A_e \tag{20}$$

Also, from the right auxiliary view,

$$\mathrm{Cos}\,\beta = \frac{E_2}{L_2} \tag{21}$$

where E_2 is obtained from Eq. (14),

$$L_2 = (E_2^2 + N^2)^{\frac{1}{2}} \tag{22}$$

$$N = (W^2 + X^2)^{\frac{1}{2}} \tag{23}$$

therefore

$$L_2 = (E_2^2 + W^2 + X^2)^{\frac{1}{2}} \tag{24}$$

By definition, the longitudinal deflection of the duct is

$$\Delta L = L_2 - L_o \tag{25}$$

From the right side and rear auxiliary views, it can be seen that

$$Y = \mathrm{Cos}\alpha \mathrm{Cos}\ A_e \tag{26}$$

$$Z = (\mathrm{Sin}^2\alpha + \mathrm{Cos}^2\alpha\ \mathrm{Sin}^2\ A_e)^{\frac{1}{2}}\ \mathrm{Cos}\ K \tag{27}$$

$$K = A_v - \epsilon \tag{28}$$

$$\epsilon = \mathrm{Sin}^{-1}\left[\frac{\mathrm{Cos}\alpha \mathrm{Sin}\ A_e}{(\mathrm{Sin}^2\alpha + \mathrm{Cos}^2\alpha\ \mathrm{Sin}^2\ A_e)^{\frac{1}{2}}}\right] \tag{29}$$

Also

$$\epsilon = \text{Cos}^{-1}\left[\frac{\text{Sin}\,\alpha}{(\text{Sin}^2\,\alpha + \text{Cos}^2\,\alpha\,\text{Sin}^2\,A_e)^{\frac{1}{2}}}\right] \tag{30}$$

Combining Eqs. (26) through (29), a simplified expression for Z was obtained as follows:

$$Z = \text{Cos}\,A_v\,\text{Sin}\,\alpha + \text{Sin}\,A_v\,\text{Sin}\,A_e\,\text{Cos}\,\alpha \tag{31}$$

Referring to the projections on the top, right auxiliary and bottom views, it can be seen that

$$\phi' = \text{Tan}^{-1}\left(\frac{R\,\text{Cos}\,\beta}{S}\right) \tag{32}$$

$$R = (Z^2 + Y^2)^{\frac{1}{2}}\,\text{Cos}\left[180-(\omega + \sigma)\right] \tag{33}$$

$$S = (Z^2 + Y^2)^{\frac{1}{2}}\,\text{Sin}\left[180-(\omega + \sigma)\right] \tag{34}$$

$$\text{Tan}\,\sigma = \frac{Z}{Y} \tag{35}$$

Combining Eqs. (32) through (34), the following relationship was obtained.

$$\phi' = \text{Tan}^{-1}\left[\frac{\text{Tan}\,\omega\,\text{Tan}\,\sigma - 1}{\text{Tan}\,\omega + \text{Tan}\,\sigma}\,\text{Cos}\,\beta\right] \tag{36}$$

Since $\phi = \phi'$ by definition of a universal joint, Eq. (7) can be written as follows.

$$\text{Tan}\,\delta = \frac{\text{Tan}\,\phi'}{\text{Cos}\,\beta} \tag{37}$$

Combining Eqs. (19), (35), (36), and (37), the following expression was obtained.

$$\text{Tan}\,\delta = \frac{WZ - XY}{XZ + WY} \tag{38}$$

The angular deflection in bending, μ, of the duct aft gimbal joint was derived with the aid of Figure A-2. Essentially, Figure A-2 is an isometric representation of the engine and pump inlet duct schematic diagram with exaggerated deflection angles. Line segment $\overline{EH}$ represents the length L_2 and position of the duct after engine gimbaling. Points E and H represent the centers of the duct forward and aft gimbal joints respectively. Triangle FGI represents the vertical plane containing the pump inlet centerline GI and a vertical line $\overline{DH}$. Triangle DEH represents the vertical plane containing the duct centerline $\overline{EH}$ and intersecting plane FGI at $\overline{DH}$. Angle μ, therefore, shows the duct aft gimbal joint angular deflection. It can be seen that

$$\overline{FG} = IG \cos A_{ev} \tag{39}$$

$$\overline{DH} = L_2 \cos \beta \tag{40}$$

By similarity of triangles FGI and DHI

$$\overline{HI} = \frac{L_2 \cos \beta}{\cos A_{ev}} \tag{41}$$

By the Law of Cosines,

$$\overline{EI}^2 = \overline{HI}^2 + \overline{EH}^2 - 2\,\overline{HI}\,\overline{EH} \cos \mu$$

or

$$\overline{EI}^2 = L_2^2 \left(\frac{\cos^2 \beta + \cos^2 A_{ev} - 2 \cos \beta \cos A_{ev} \cos \mu}{\cos^2 A_{ev}} \right) \tag{42}$$

Also,

$$\overline{ED} = L_2 \sin \beta \tag{43}$$

$$\overline{EF} = L_2 \sin \beta \sin \eta \tag{44}$$

$$\overline{IF} = \overline{IG} \sin A_{ev} \tag{45}$$

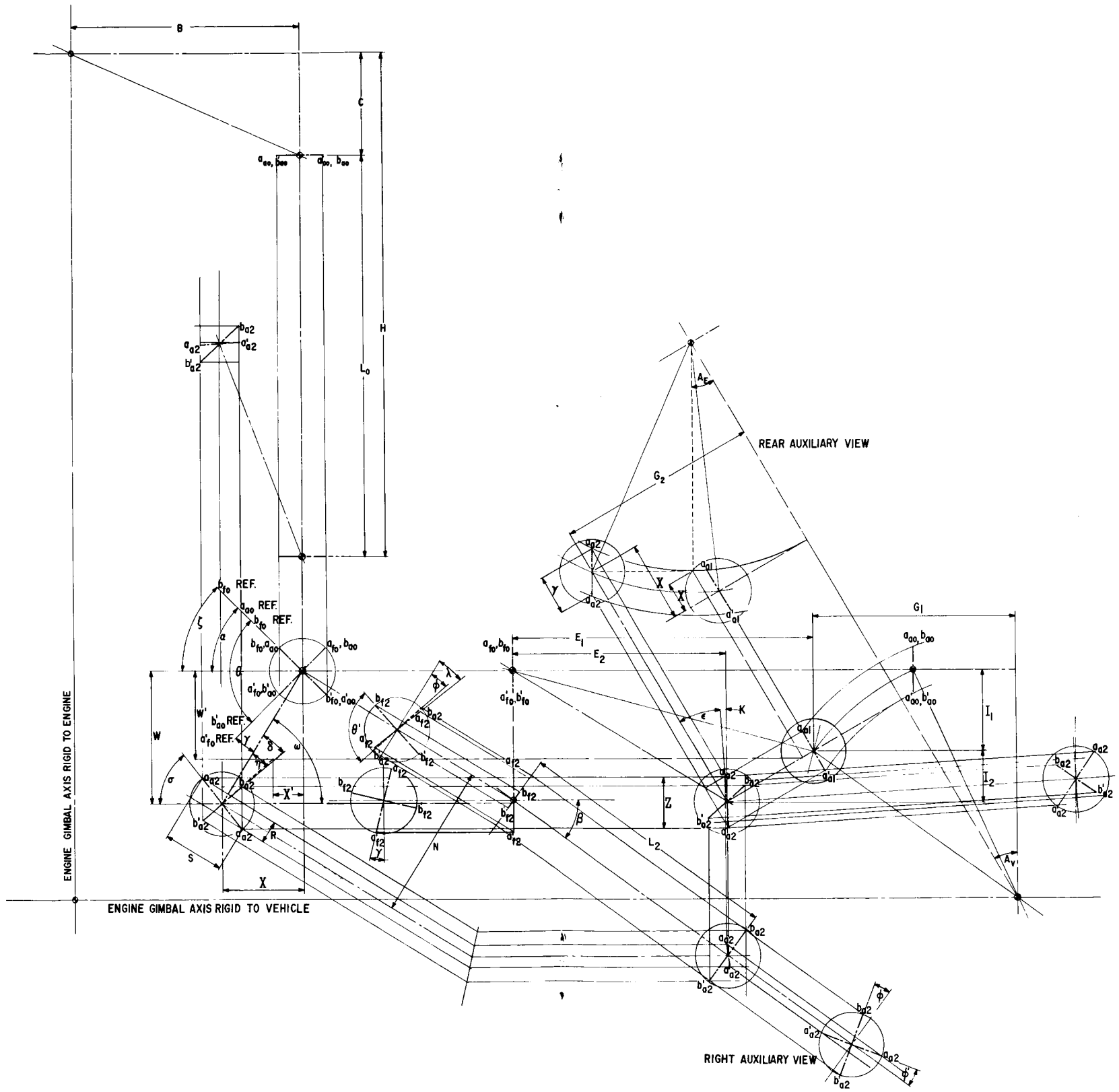

FIGURE A-1 KINEMATIC DIAGRAM DRAWING 20SK96

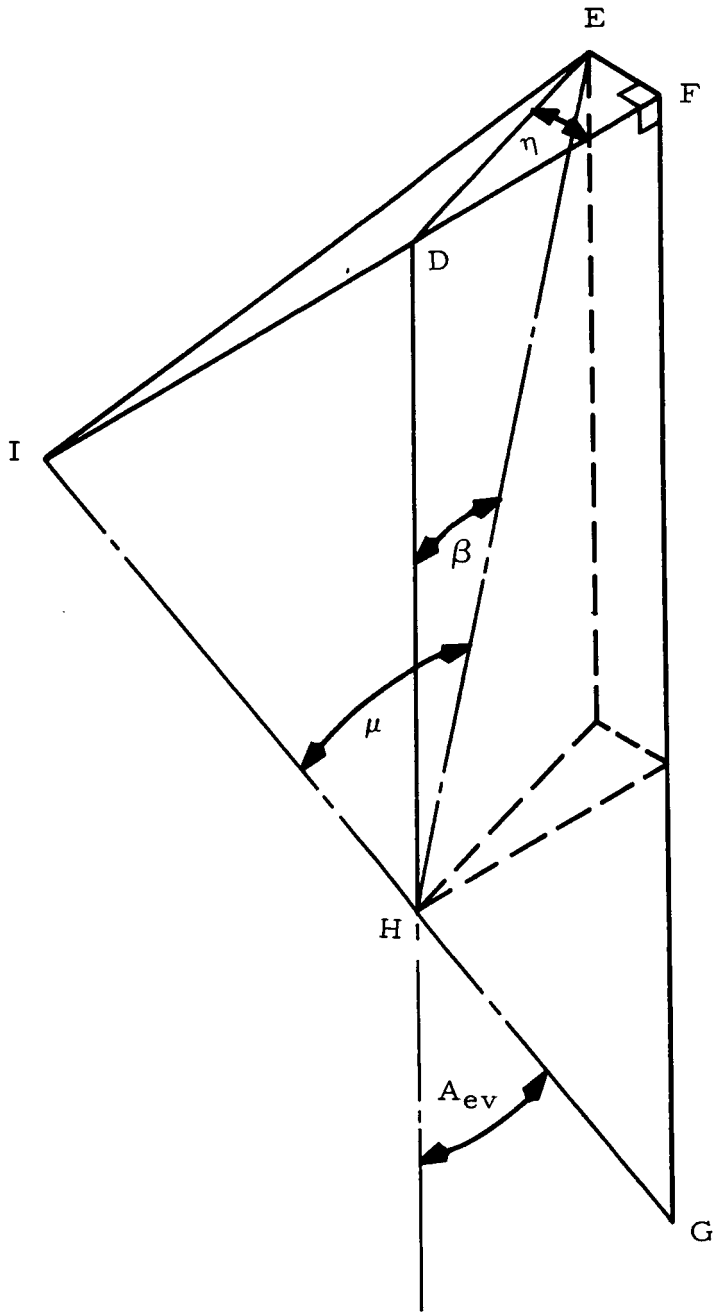

FIGURE A-2. PUMP INLET AND DUCT SCHEMATIC DIAGRAM (ISOMETRIC)

therefore,

$$\overline{EI}^2 = \overline{IF}^2 + \overline{EF}^2$$

or $$\overline{EI}^2 = \overline{IG}^2 \text{Sin}^2 A_{ev} + L_2^2 \text{ Sin}^2 \beta \text{ Sin}^2 \eta \quad (46)$$

Also, $$\overline{DF} = L_2 \text{ Sin}\beta \text{ Cos}\eta \quad (47)$$

$$\overline{DI} = \overline{HI} \text{ Sin } A_{ev} \quad (48)$$

Combining Eqs. (41), (45), (47), and (48)

$$\overline{IG} = L_2 \left(\frac{\text{Cos}\,\beta}{\text{Cos } A_{ev}} + \frac{\text{Sin}\,\beta}{\text{Sin } A_{ev}} \text{ Cos}\eta \right) \quad (49)$$

Combining Eqs. (42), (46), and (49), the general expression for μ was obtained

$$\mu = \text{Cos}^{-1}(\text{Cos}\,\beta \text{ Cos } A_{ev} - \text{Sin}\,\beta \text{ Sin } A_{ev} \text{ Cos}\eta) \quad (50)$$

The resultant gimbal angle, A_{ev}, was expressed in terms of the gimbal angle components A_e and A_v with the aid of Figure A-3. Consider the geometric axis of the engine thrust chamber as contained in line $\overline{OA}$ when at zero gimbal position; in line $\overline{OB}$ after rotation by an angle A_e; and in line $\overline{OC}$ after rotation by an angle A_v from line $\overline{OB}$. It can be seen that

$$\overline{OA} = \overline{OB} \text{ Cos } A_e \quad (51)$$

$$\overline{OA} = \overline{OC} \text{ Cos } A_{ev} \quad (52)$$

$$\overline{OB} = \overline{OC} \text{ Cos } A_v \quad (53)$$

Combining Eqs. (51) through (53)

$$A_{ev} = \text{Cos}^{-1} (\text{Cos } A_e \text{ Cos } A_v) \quad (54)$$

The angle, η, between the horizontal components of the duct longitudinal axis and pump inlet centerline was expressed in terms

of the system parameters and variables as follows. Referring back to Figure A-1, it can be seen that

$$W' = B_v (1 - \text{Cos } A_v) + B_e \text{ Sin } A_e \text{ Sin } A_v \tag{55}$$

$$X' = B_e (1 - \text{Cos } A_e) \tag{56}$$

therefore

$$\text{Tan } (\omega - \eta) = \frac{W - W'}{X - X'} \tag{57}$$

Combining Eqs. (18), (20), (55), (56), and (57)

$$\text{Tan } (\omega - \eta) = \frac{\text{Sin } A_v \text{ Cos } A_e}{\text{Sin } A_e} \tag{58}$$

or

$$\eta = \omega - \text{Tan}^{-1} \left(\frac{\text{Sin } A_v}{\text{Tan } A_e} \right)$$

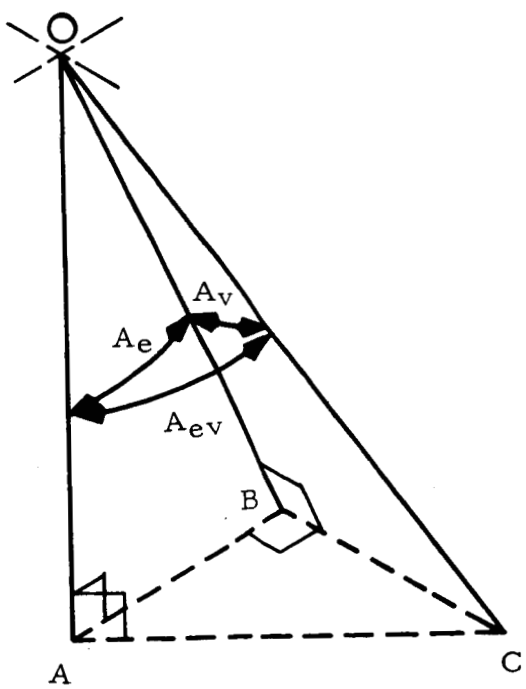

FIGURE A-3. COMPOUND ANGLE

APPENDIX B

DEFLECTION CURVES OF THE PUMP INLET DUCTS DUE TO ENGINE GIMBAL MOVEMENTS IN THE S-IC STAGE

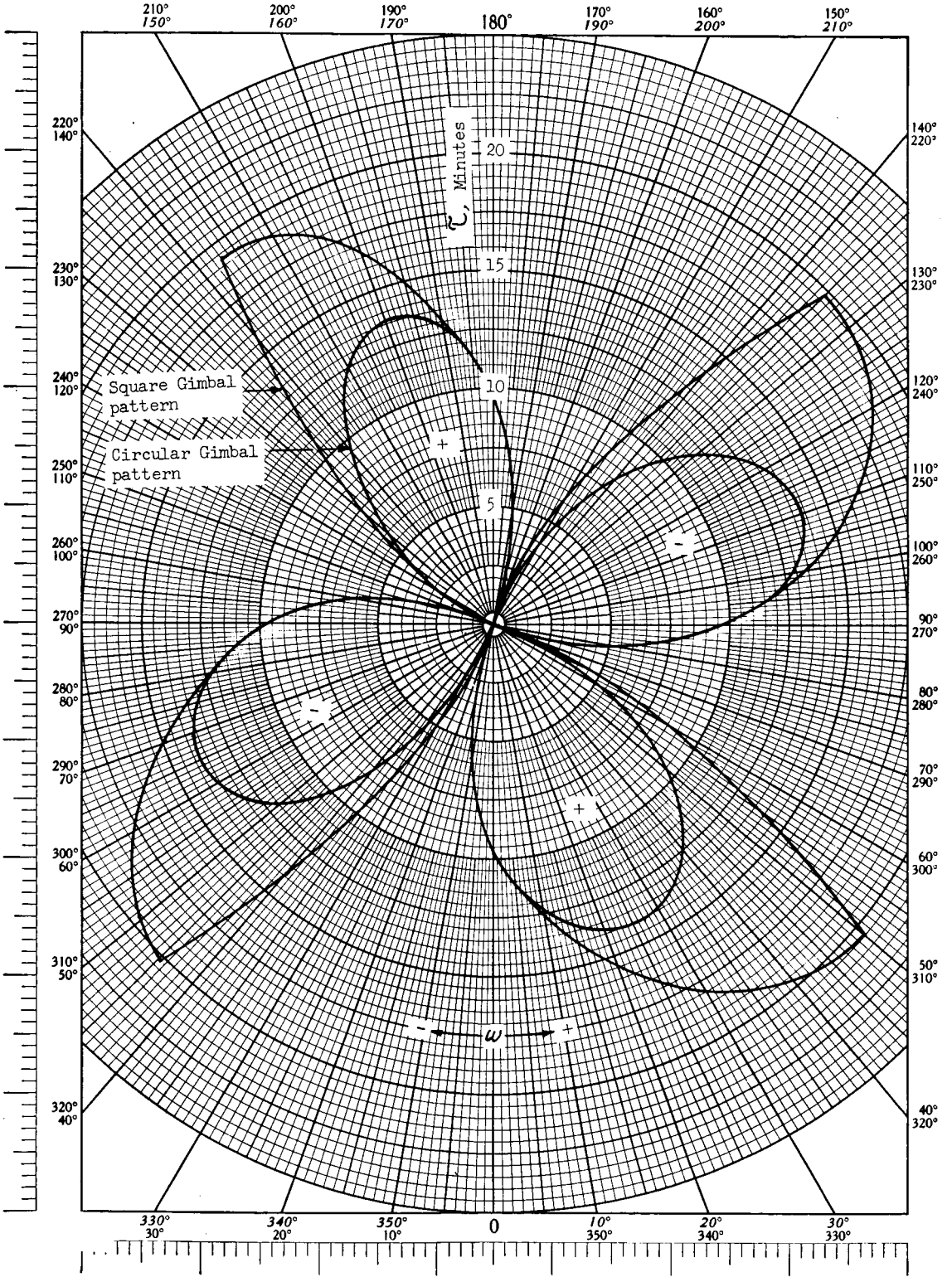

FIGURE B-1 TORSIONAL DEFLECTION τ OF LOX DUCT VERSUS ω FOR α = + 45 AND ζ = -15

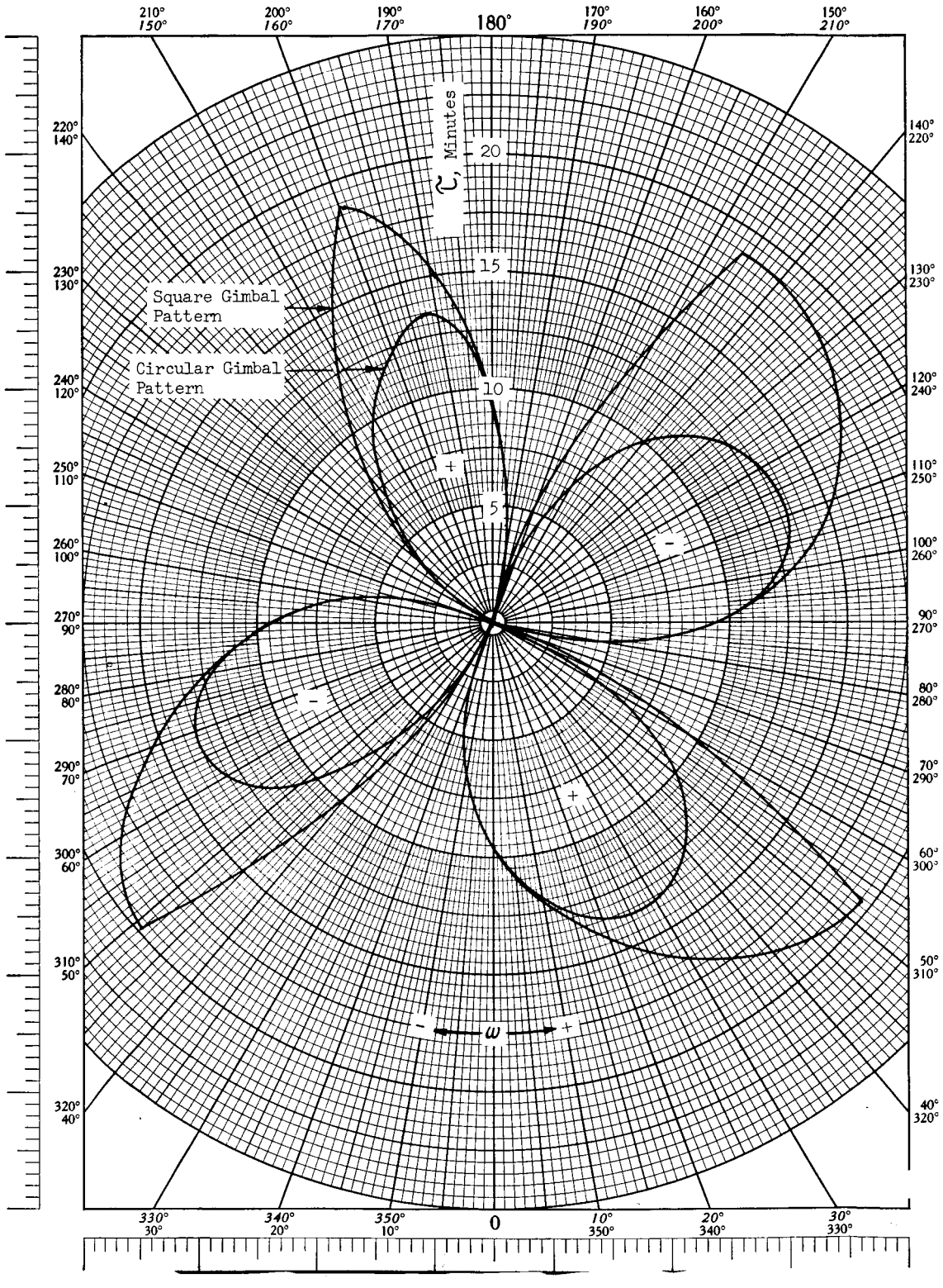

FIGURE B-2 TORSIONAL DEFLECTION τ OF FUEL DUCT NO. 1 VERSUS ω FOR α = +45 AND ζ = -15

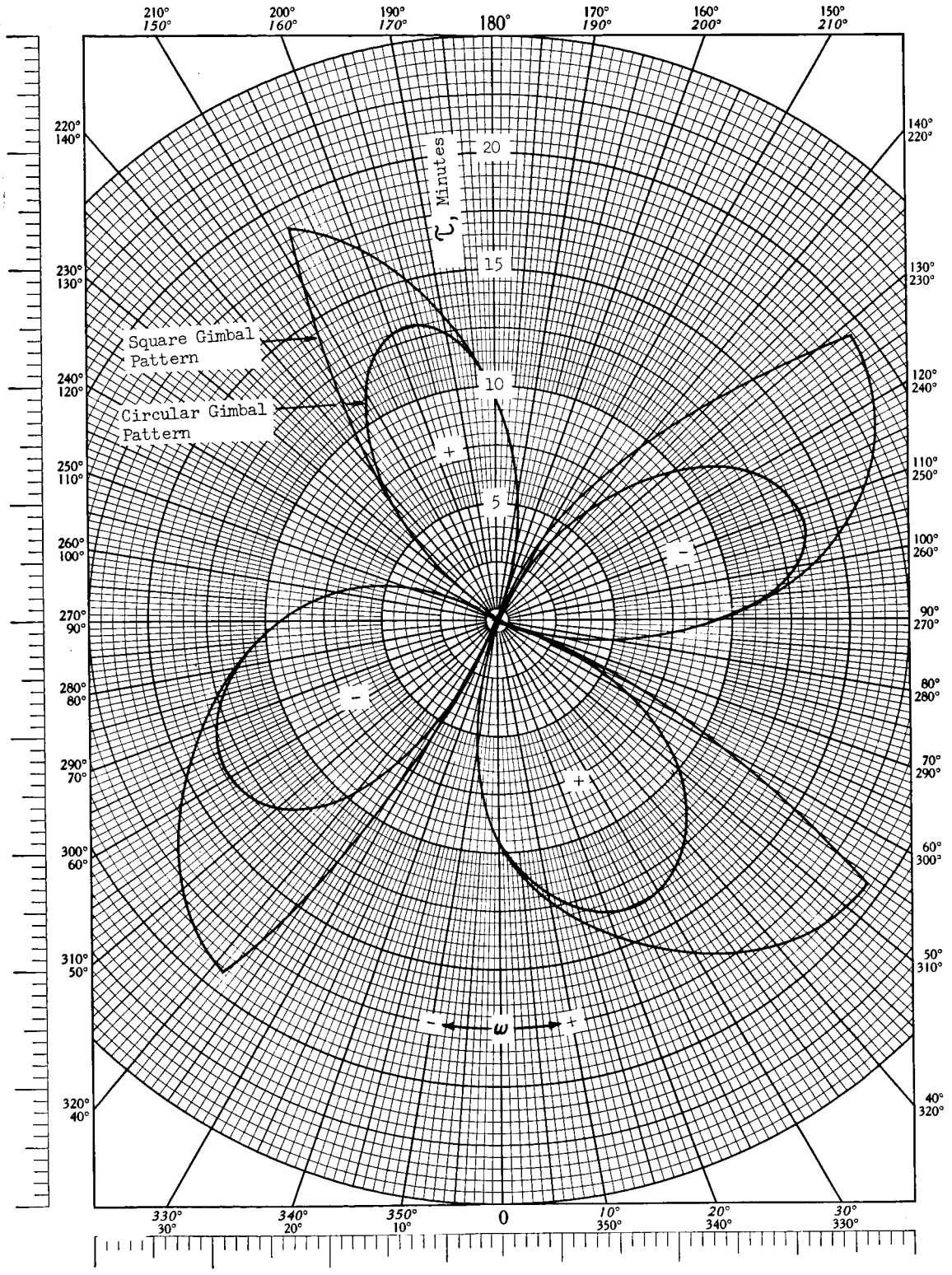

FIGURE B-3 TORSIONAL DEFLECTION τ OF FUEL DUCT NO. 2 VERSUS ω FOR α = +45 AND ζ = -15

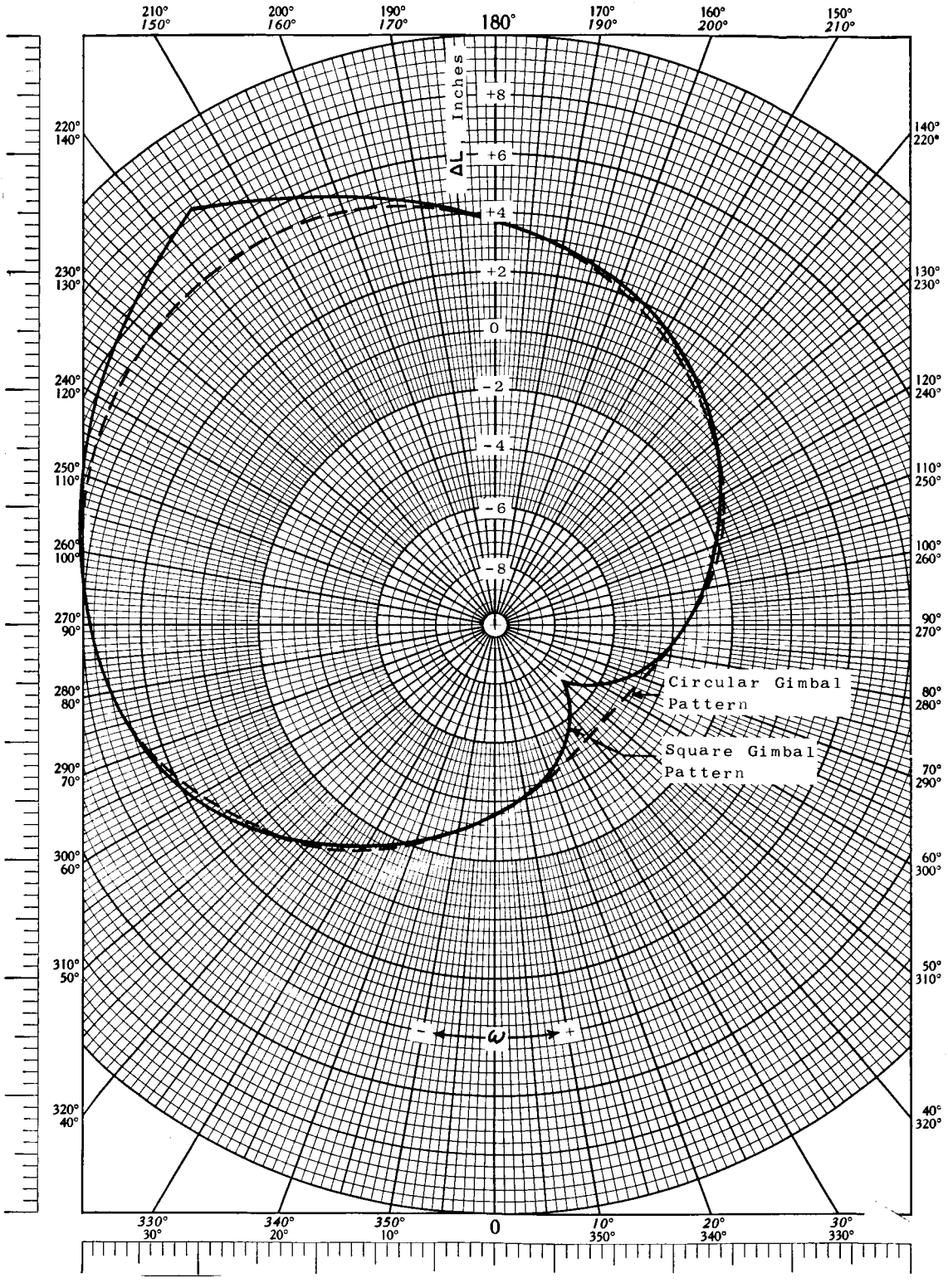

FIGURE B-4 CHANGE IN LENGTH ΔL OF LOX DUCT VERSUS ω

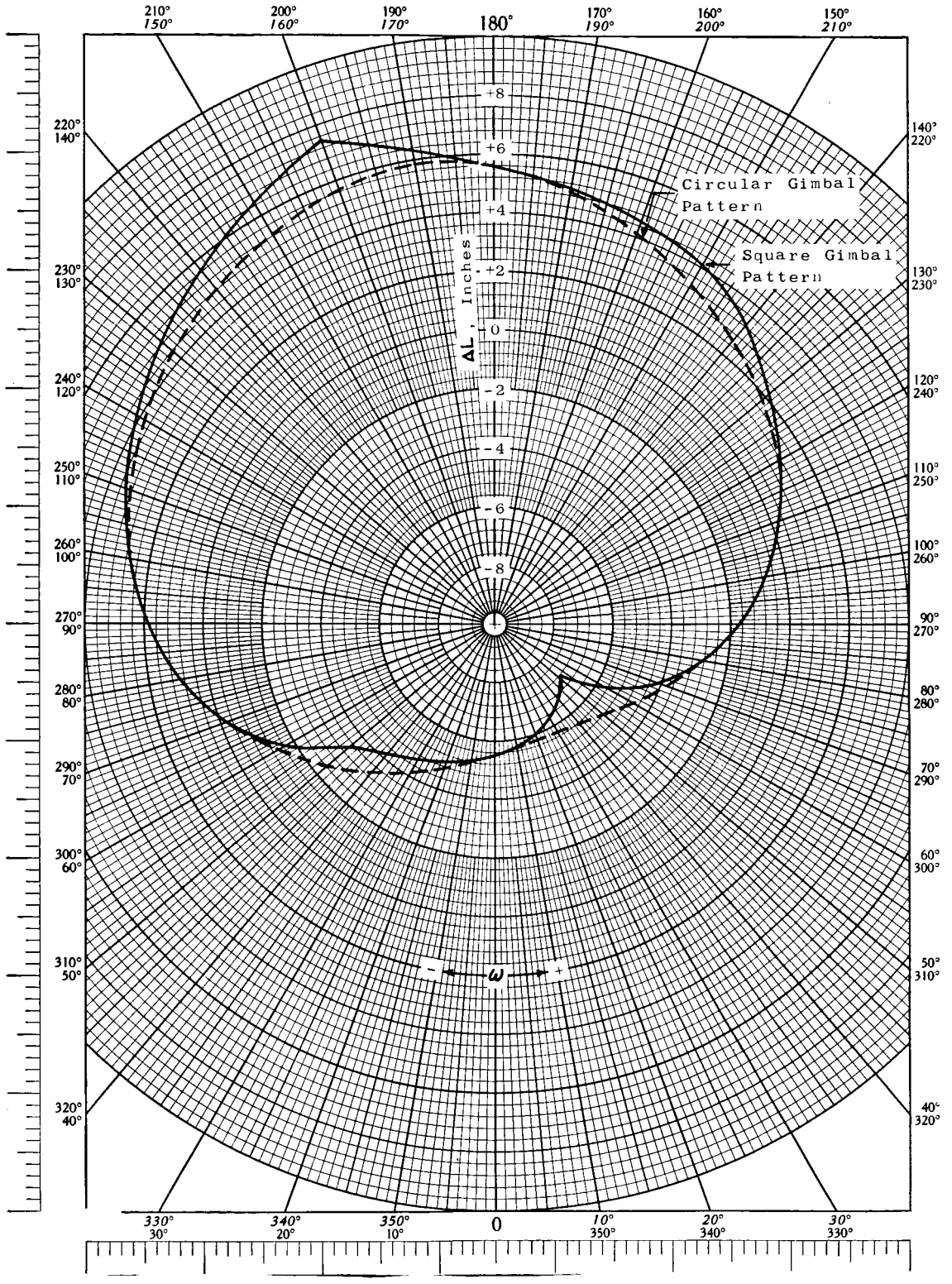

FIGURE B-5 CHANGE IN LENGTH ΔL OF FUEL DUCT NO. 1 VERSUS ω

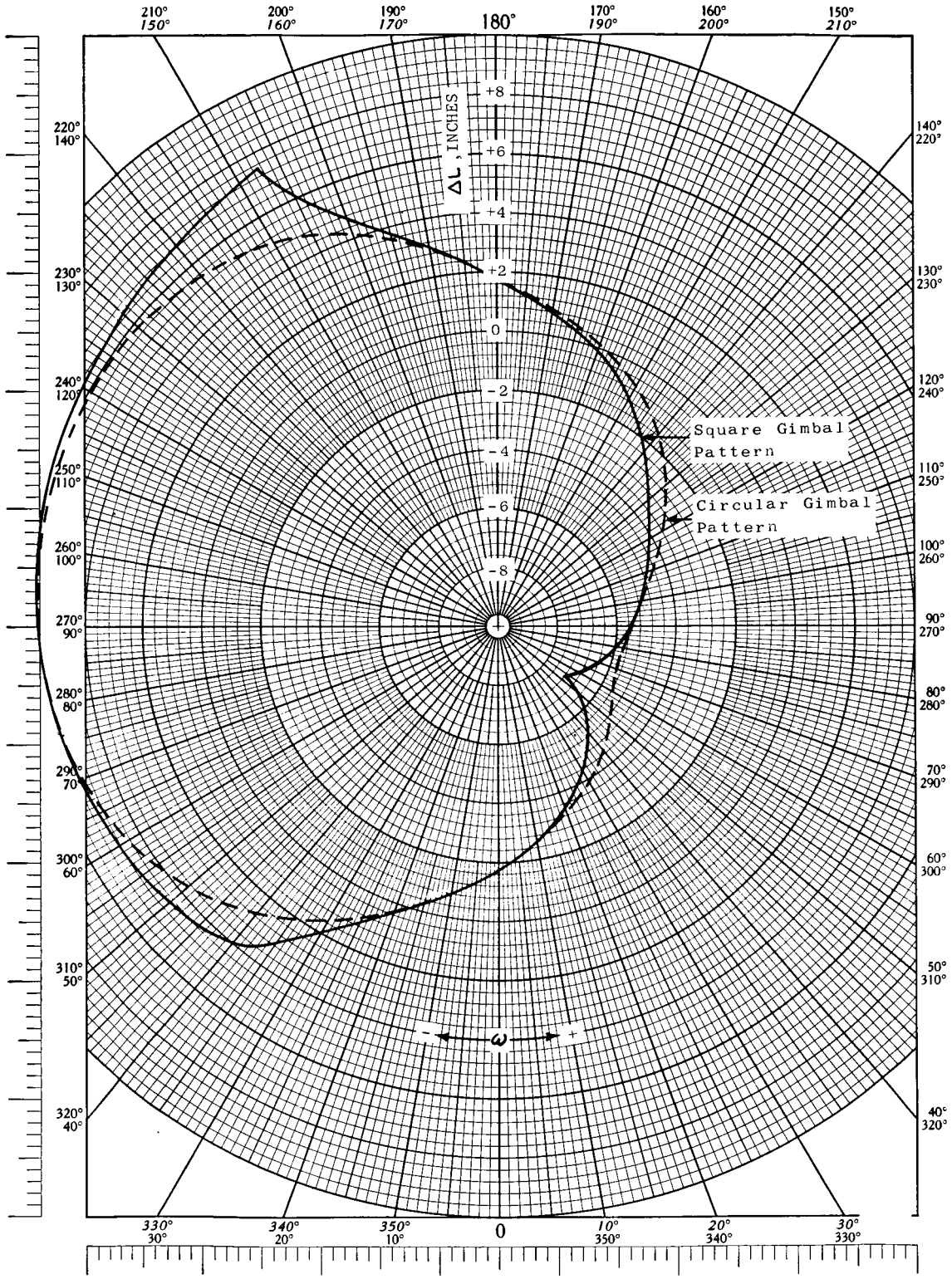

FIGURE B-6 CHANGE IN LENGTH ΔL OF FUEL DUCT NO. 2 VERSUS ω

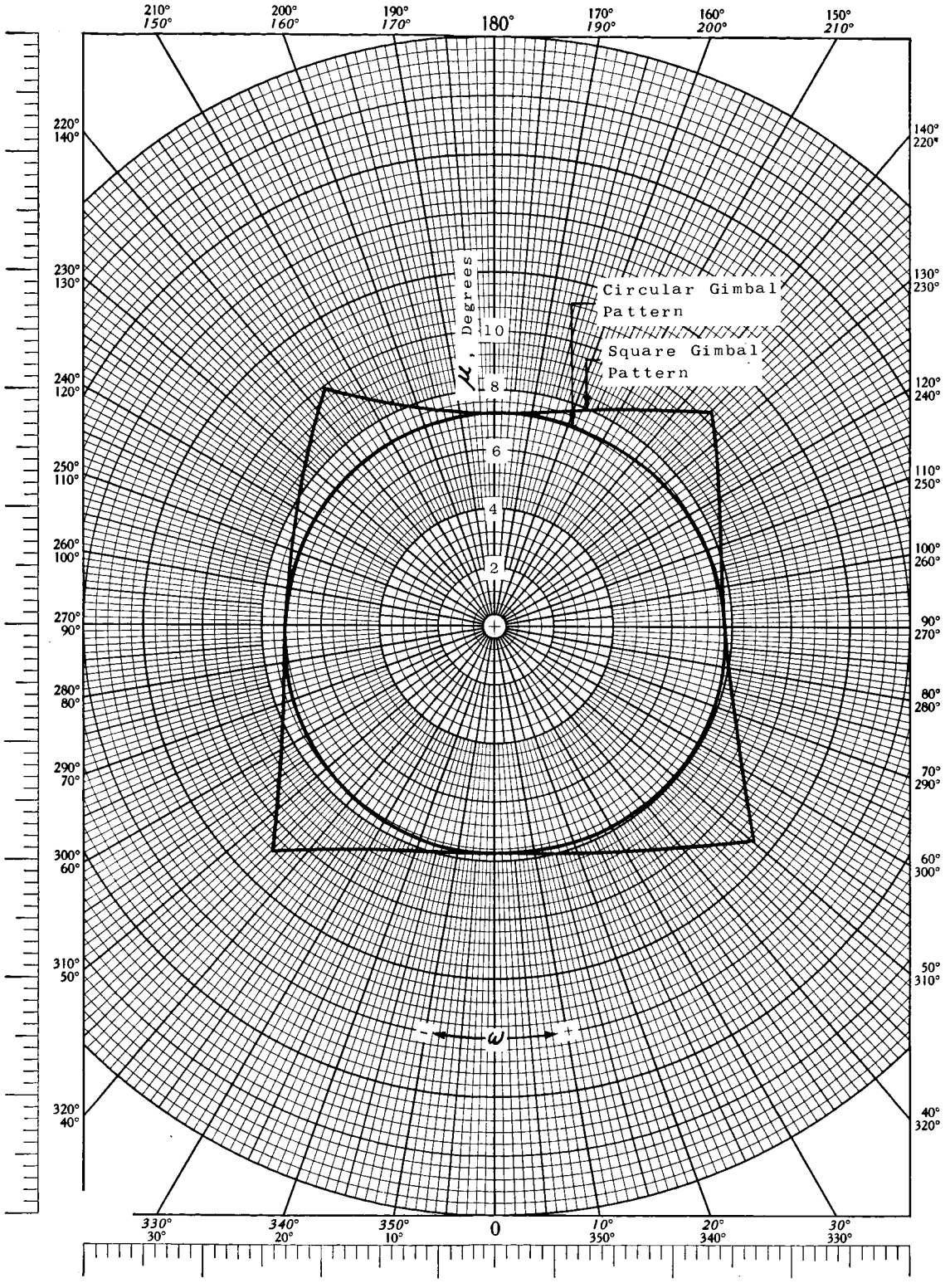

FIGURE B-7 ANGULAR DEFLECTION μ OF LOX DUCT AFT GIMBAL JOINT VERSUS ω

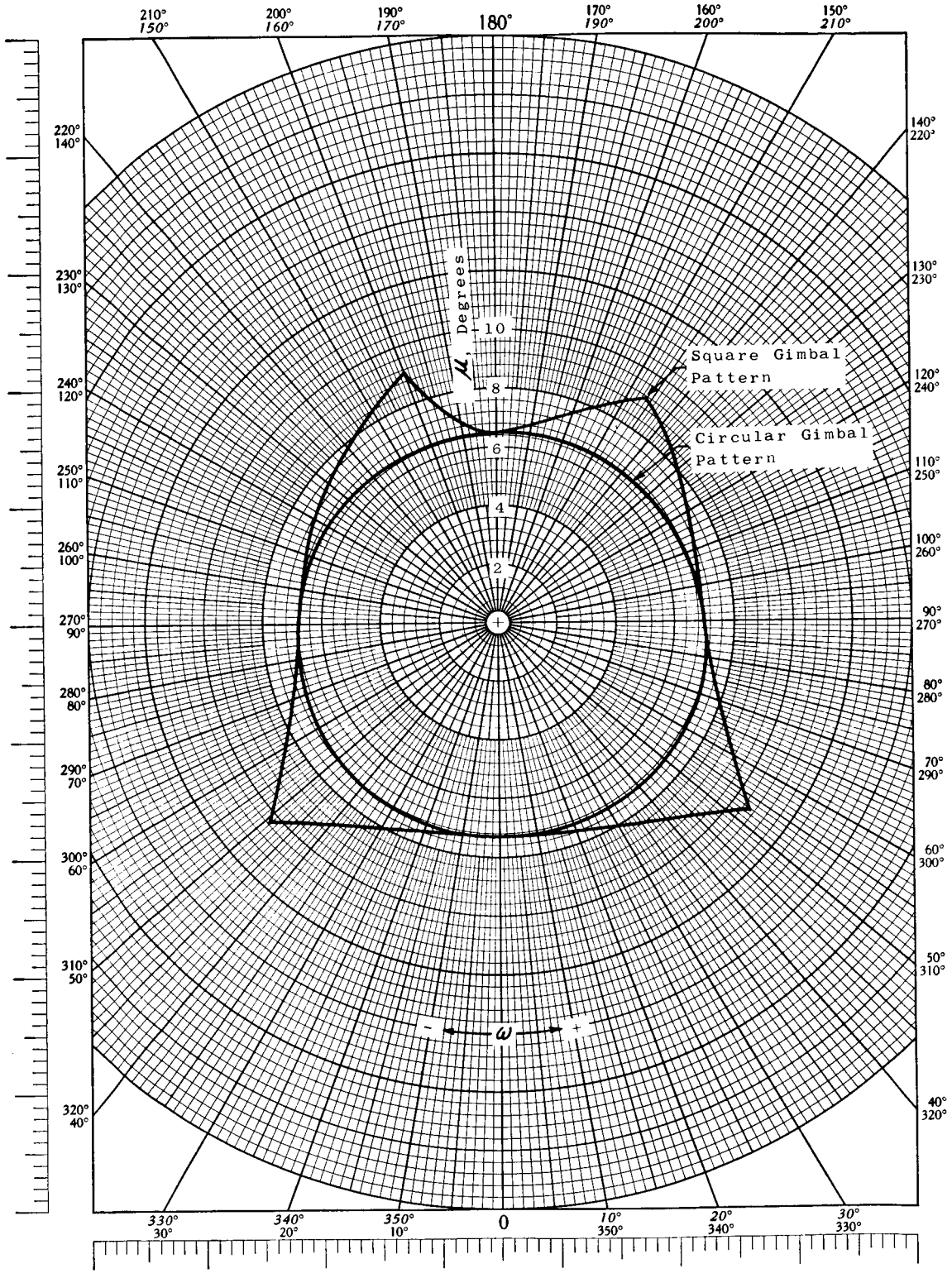

FIGURE B-8 ANGULAR DEFLECTION μ OF FUEL DUCT NO. 1 AFT GIMBAL JOINT VERSUS ω

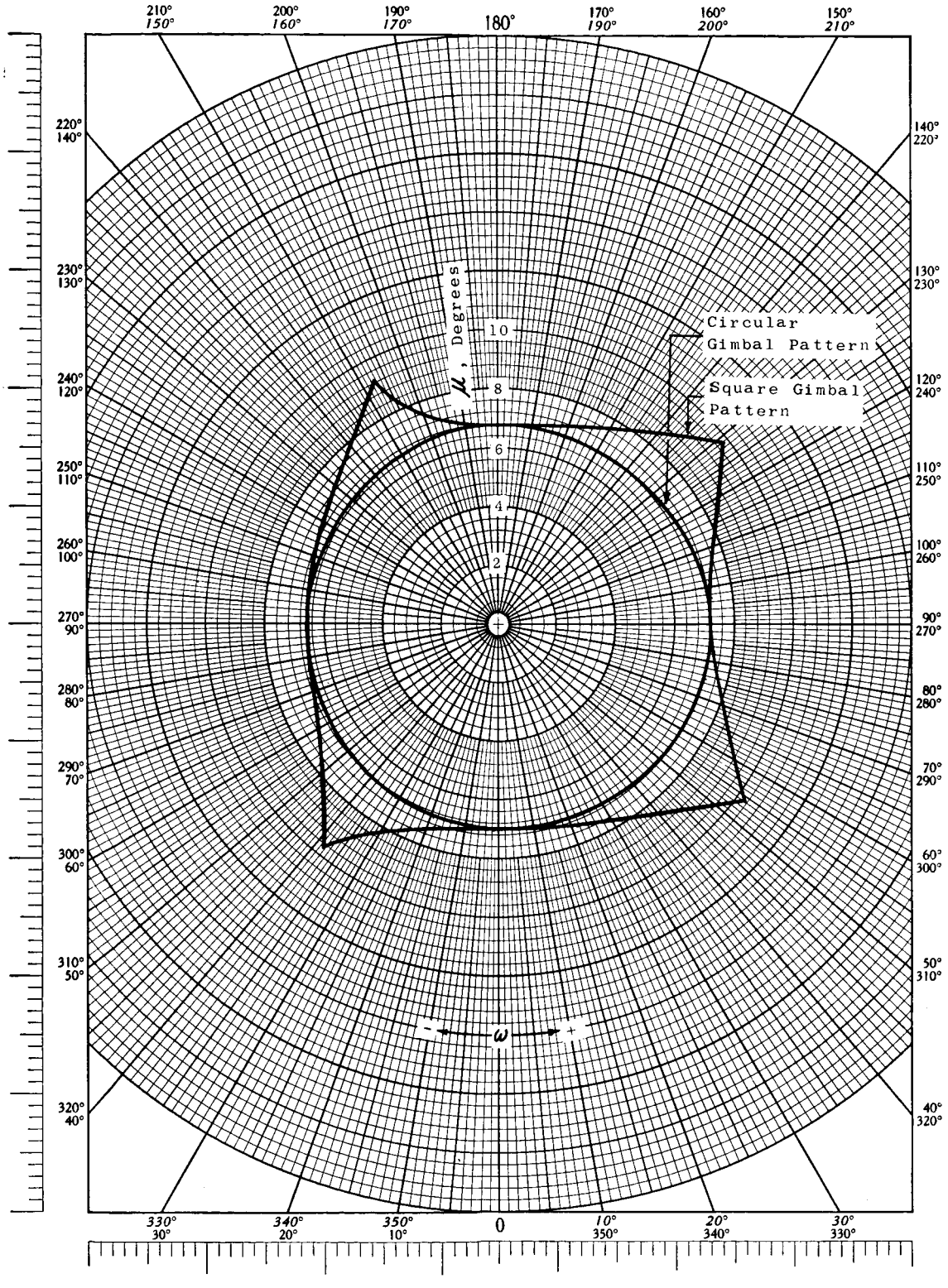

FIGURE B-9 ANGULAR DEFLECTIONS μ OF FUEL DUCT NO. 2 AFT GIMBAL JOINT VERSUS ω

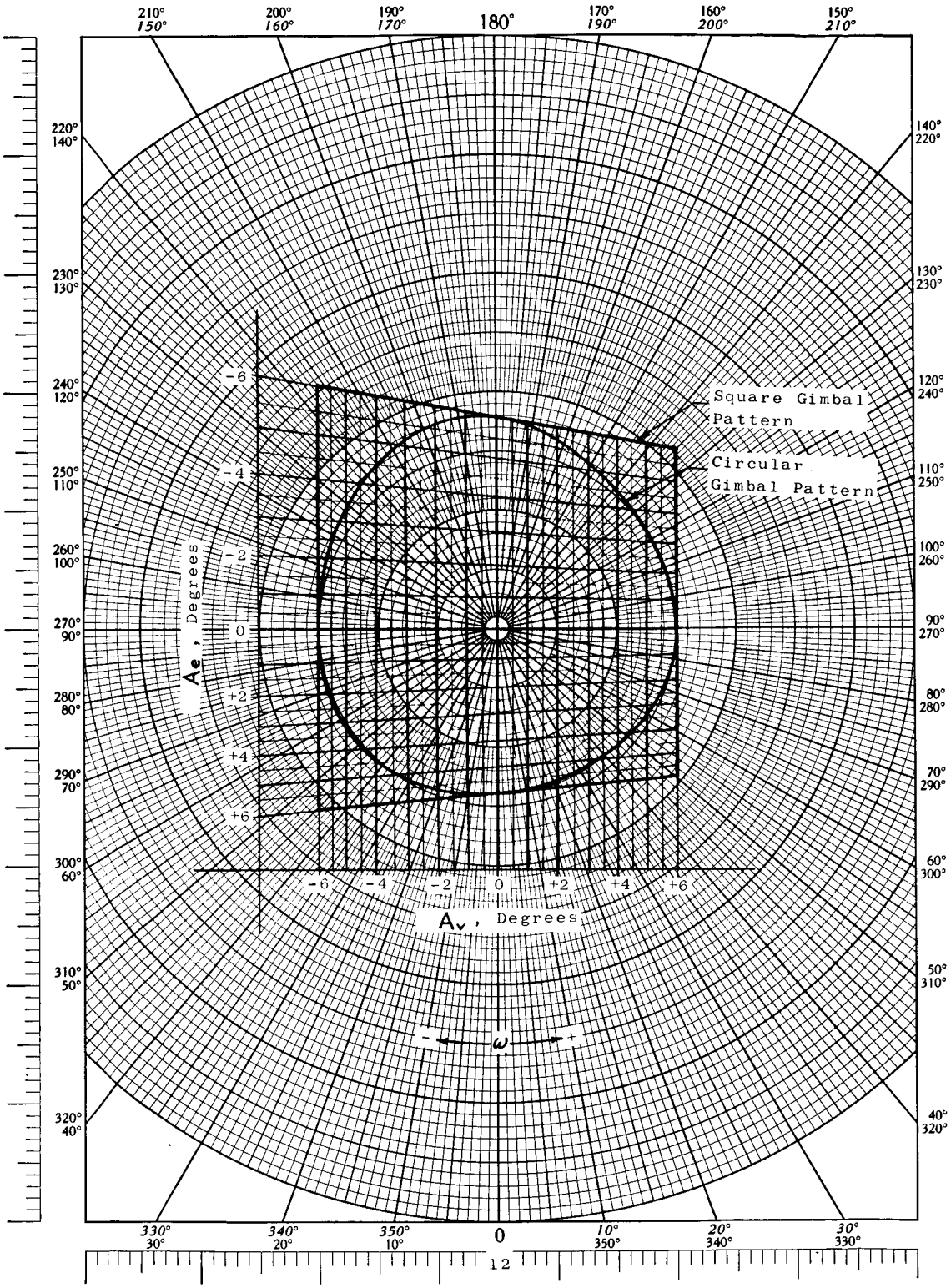

FIGURE B-10 ENGINE GIMBAL ANGLE VERSUS ω FOR LOX PUMP INLET

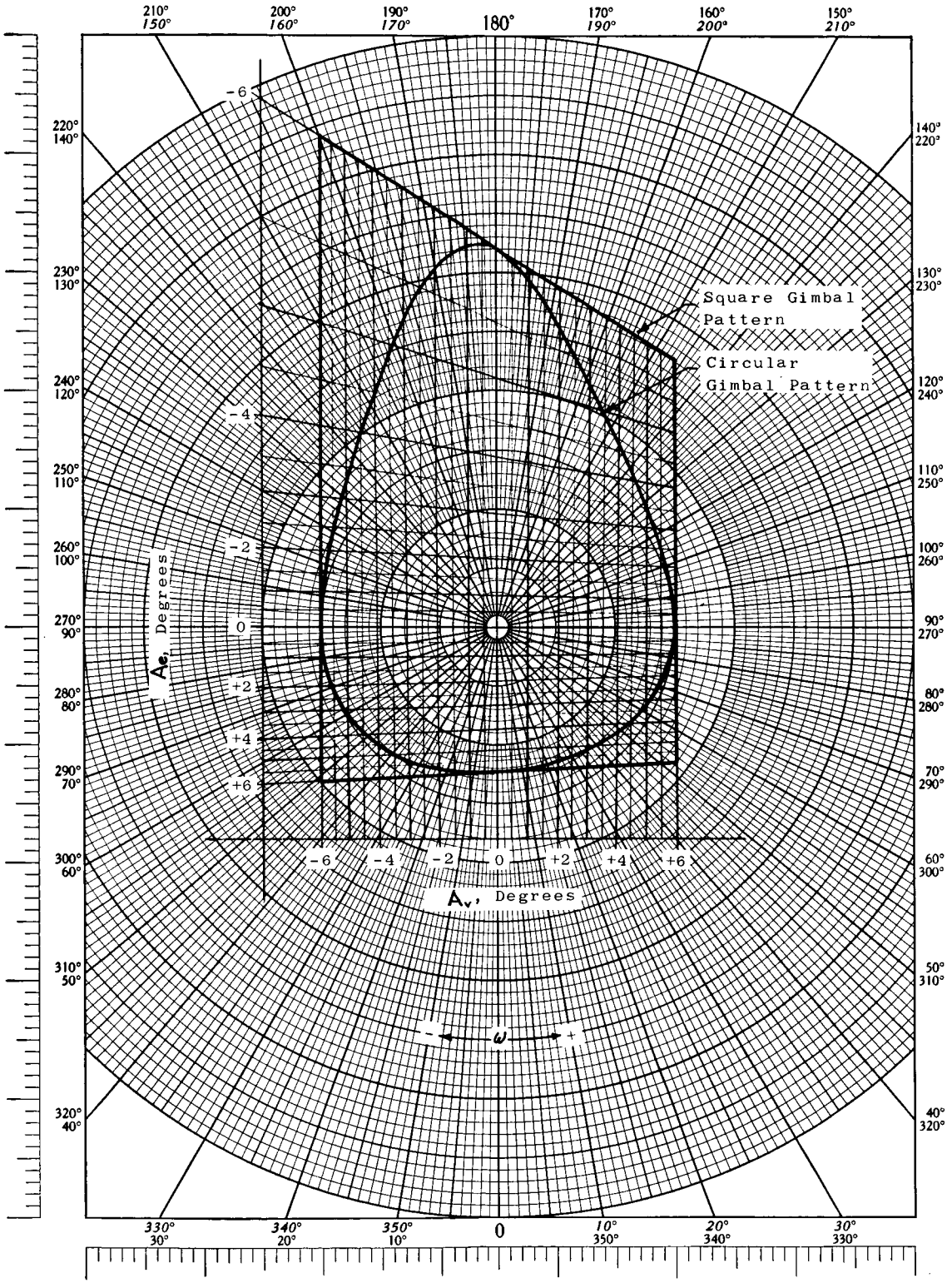

FIGURE B-11 ENGINE GIMBAL ANGLE VERSUS ω FOR FUEL PUMP INLET NO. 1

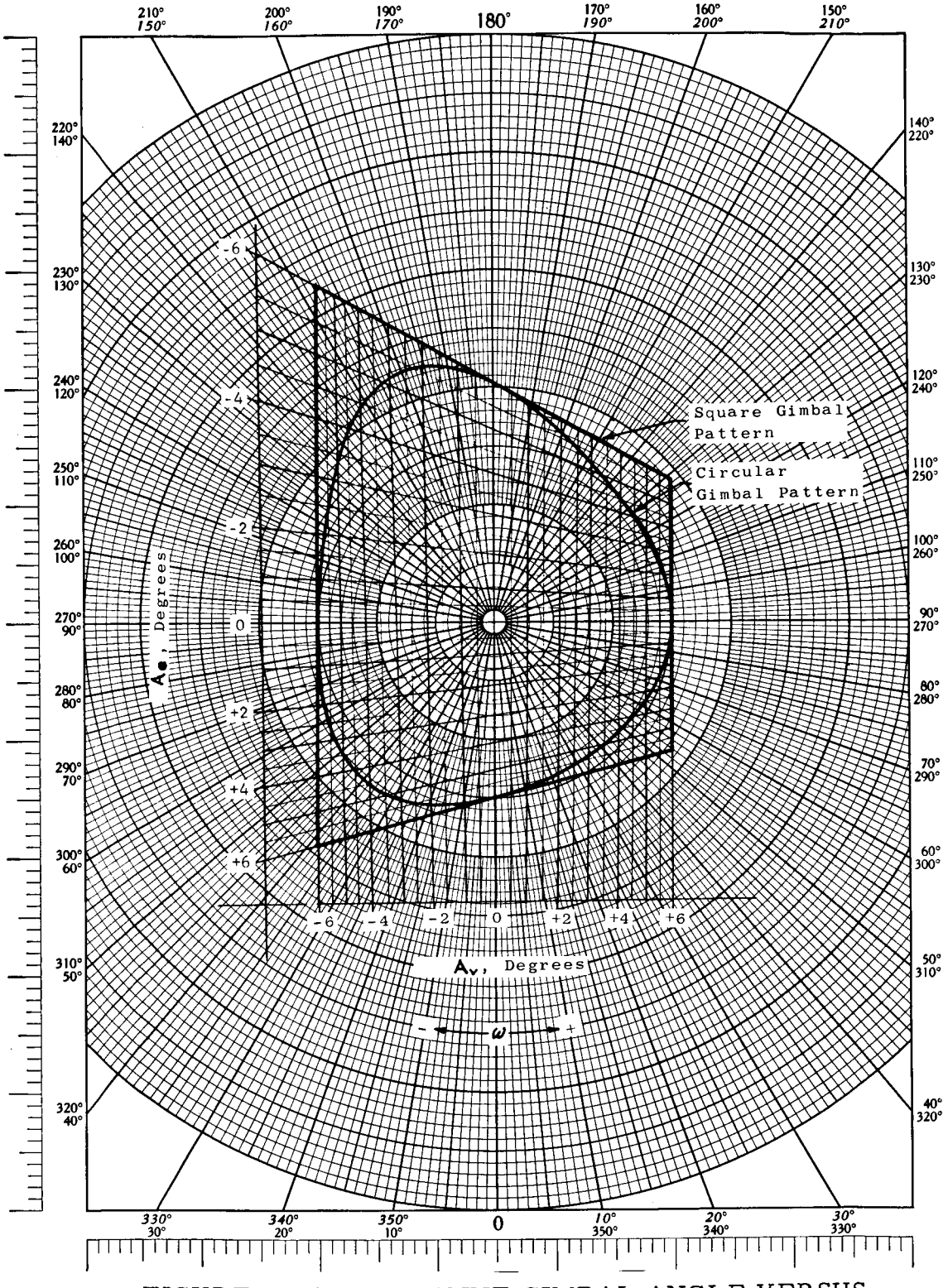

FIGURE B-12 ENGINE GIMBAL ANGLE VERSUS ω FOR FUEL PUMP INLET NO. 2

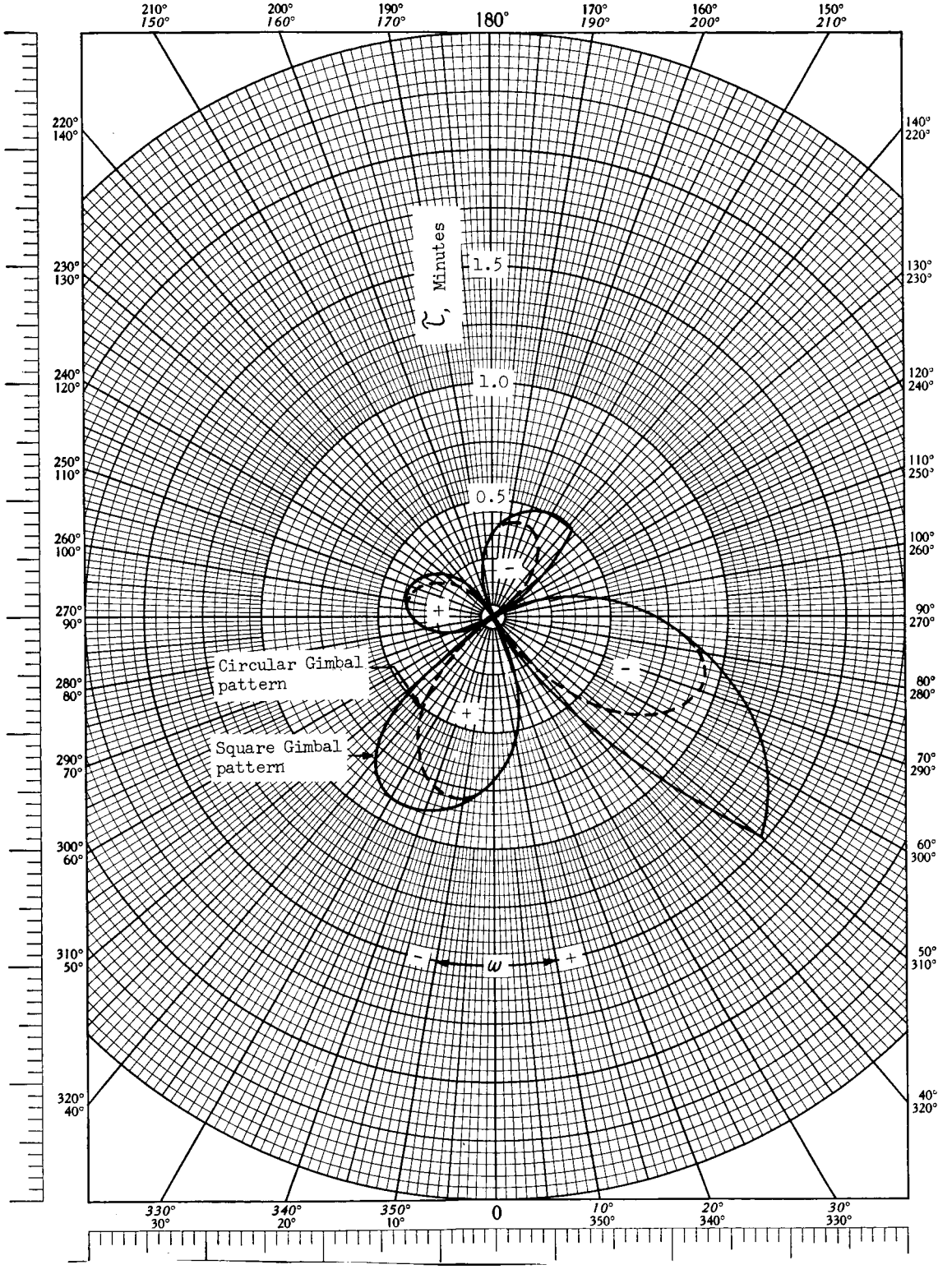

FIGURE B-13 TORSIONAL DEFLECTION τ OF LOX DUCT VERSUS ω FOR α = +90 AND ζ = +30 DEGREES

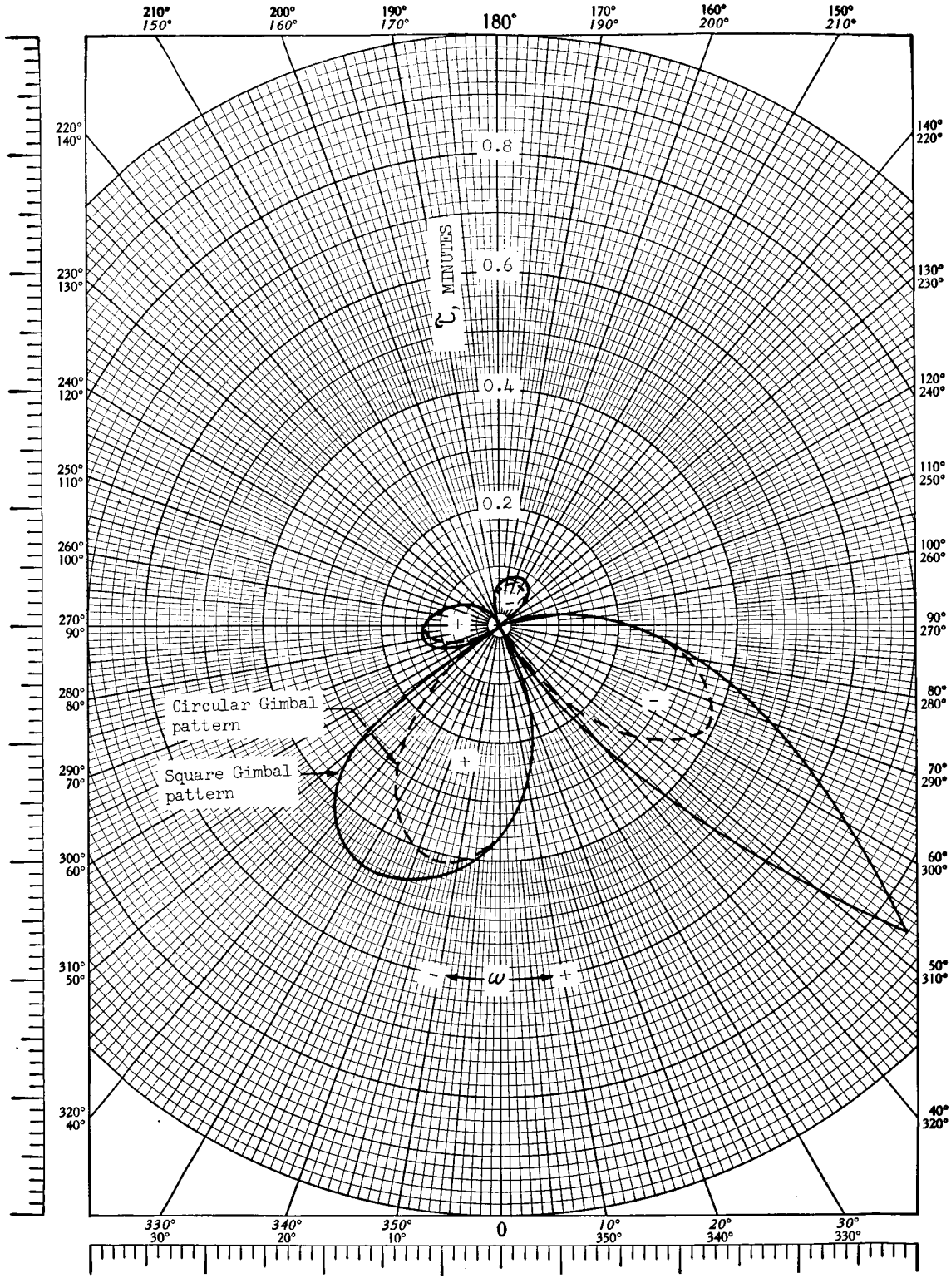

FIGURE B-14 TORSIONAL DEFLECTION τ OF FUEL DUCT NO. 1 VERSUS ω FOR α = +90 AND ζ = +30 DEGREES

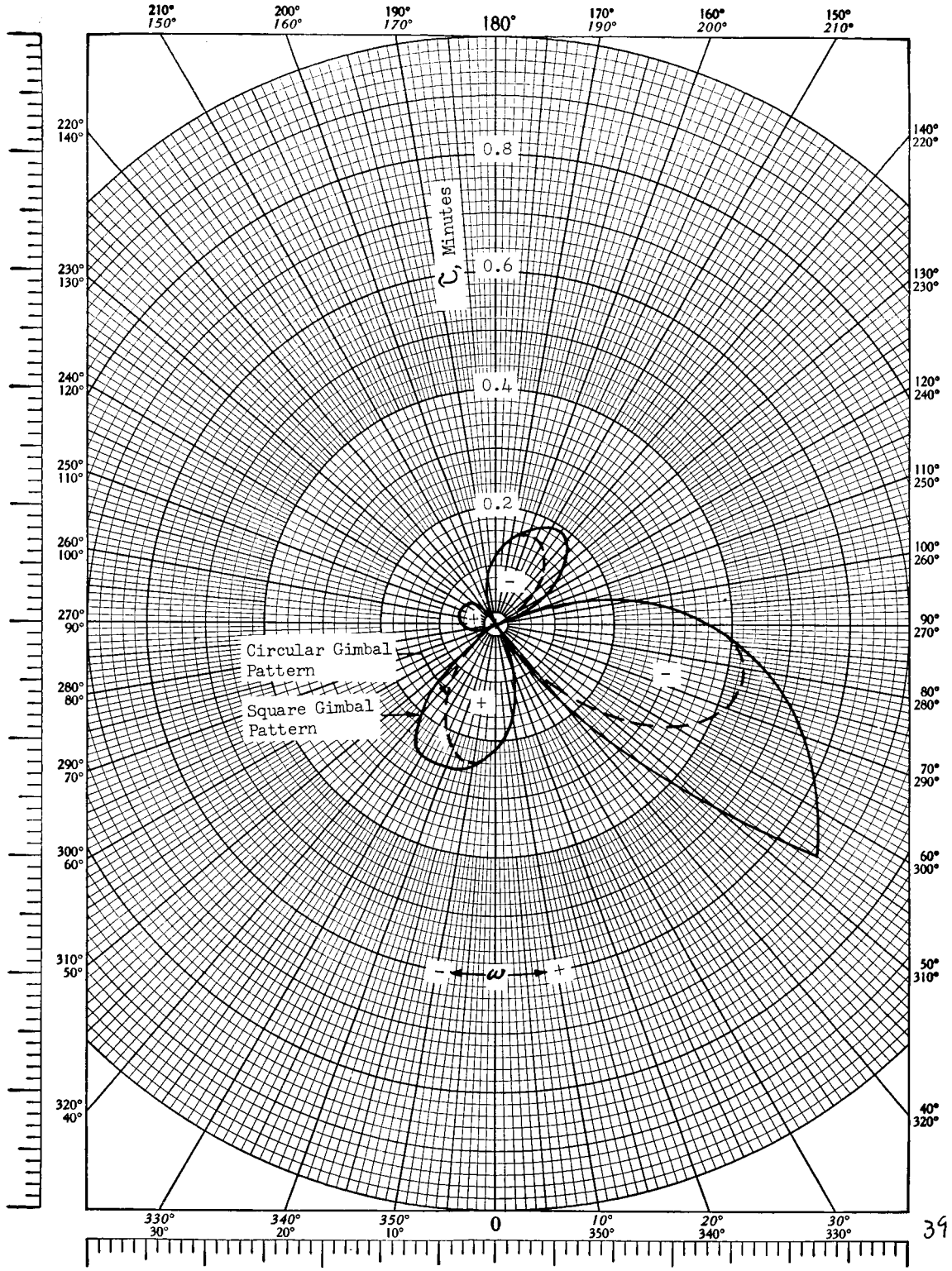

FIGURE B-15 TORSIONAL DEFLECTION τ OF FUEL DUCT NO. 2 VERSUS ω FOR α = +90 AND ζ = +30 DEGREES

REFERENCES

1. Memo R-P&VE-PA-288-63, Kinematic Analysis of the F-1 Engine and Pump Inlet Duct Gimbal Joint System, January 3, 1964.

2. MSFC Specification No. 20M02000; Duct, Outboard LOX, Pressure-Volume Compensator.

3. Arrowhead Products Drawing No. 11711; Duct, Outboard LOX, Pressure-Volume Compensator.

4. MSFC Specification No. 20M02001; Duct, Outboard Fuel, Pressure-Volume Compensator.

5. Arrowhead Products Drawing No. 11713; Duct, Outboard Fuel, Pressure-Volume Compensator.

6. Rocketdyne Drawing No. 104011, Dimensions-Customer connections, F-1 (C)

7. MSFC Specification Control Drawing No. 60B41149-65, Seal-NAFLEX.

8. MSFC Specification Control Drawing No. 60B43062-33, Seal-GASK-O.

NASA-Langley, 1964 M318